

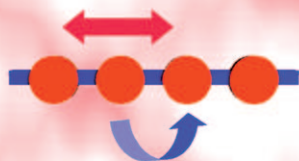
Conducting Polymer Networks Cross-Linked by "Isolated" Functional Dyes: Design, Synthesis, and Electrochemical Polymerization of Doubly Strapped Light-Harvesting Porphyrin/Oligothiophene Monomers

Kazunori Sugiyasu* and Masayuki Takeuchi*[a]

Dedicated to Professor Seiji Shinkai on the occasion of his 65th birthday

Dye-Functionalized Conducting Polymers

● Dyes on Backbone



● Dyes at Sidechains



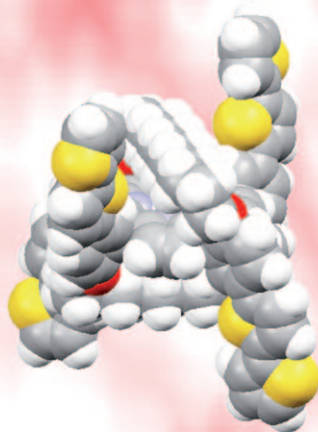
Desired:

Effective electronic interaction such as energy and/or electron transfer, etc.

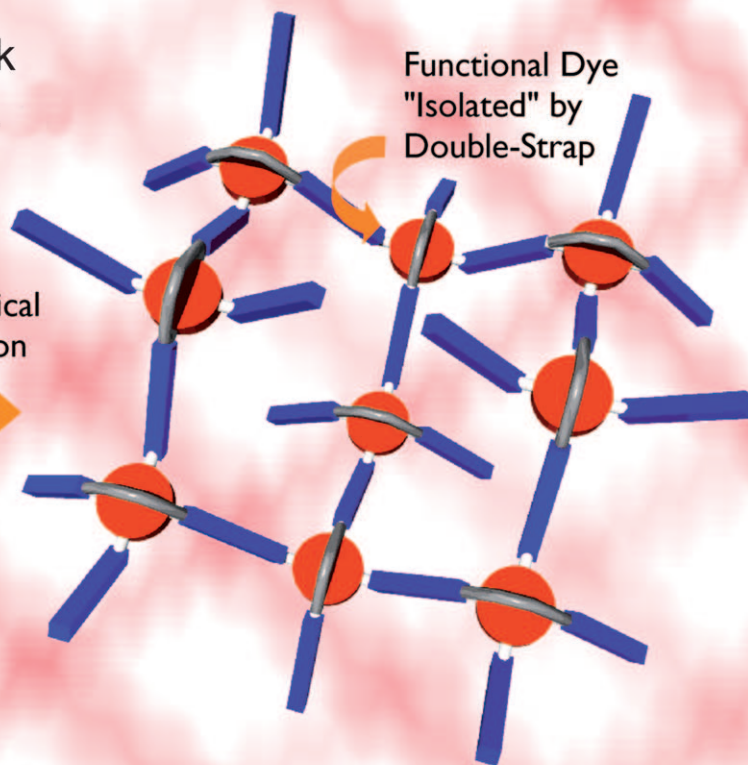
Undesired:

Aggregation that causes, for example, excimer formation, charge trap, etc.

● "Isolated" Dyes in Network can address the tradeoff.



Electrochemical
Polymerization



Abstract: We have synthesized doubly strapped porphyrin derivatives with four bithiophene segments that diverge from the porphyrin core, namely, **Por(BT)₄** and **PorZn(BT)₄**. These molecules are designed as electrochemically polymerizable monomers that will yield the highly cross-linked conducting polymeric networks **poly[Por(BT)₄]** and **poly[PorZn(BT)₄]**, respectively, through an oxidative coupling reaction among the bithiophene moieties. Selective synthesis of the distal doubly strapped porphyrin derivatives was successful from the bis(formylphenyl) and bis(dipyrrolylmethylphenyl) straps under Lindsey conditions. Slow kinetics observed for the zinc insertion reaction toward the doubly strapped porphyrin derivative revealed that both faces of the porphyrin plane are overlaid with alkyl chain straps. To probe this “isolation” effect, photophysical properties

of the monomers and their model components were investigated by UV/Vis and fluorescence spectroscopic analysis. An absorption spectral comparison between the diluted solution and the thin solid film of **Por(BT)₄** demonstrated that the porphyrin molecule is shielded by the double strap and self-aggregation is prevented. It is noteworthy that the fluorescence of the spin-coated film of the doubly strapped porphyrin monomer was twice as strong as that of an unstrapped porphyrin, thus indicating that the double strap can suppress undesired deactivation processes from the photoexcited state. In addition, fluorescence spectral measurements revealed that quantitative energy transfer from

the oligothiophene segments to the porphyrin molecule takes place, which demonstrates an effective electronic interaction between these two chromophores. Electrochemical polymerization of the monomers **Por(BT)₄** and **PorZn(BT)₄** gave robust films that showed stable electrochemistry. Absorption spectral measurements and electrochemical characterization of the obtained films showed that the doubly strapped porphyrins are incorporated into the conducting polymer networks without any decomposition and protonation. Given all these observations above, our new monomer design based on functional dyes shielded by the double strap will lead to new organic optoelectronic materials in which functional molecules are spatially incorporated and isolated and yet show an effective electronic interactions with the conducting polymer backbones.

Keywords: conducting materials • energy transfer • light-harvesting • polythiophenes • porphyrins

Introduction

Conducting polymers are the most promising materials in the field of future electronics as an alternative to inorganic counterparts due to their tunable optoelectronic properties and rich advantages endowed as an organic substance (flexible, processible, and lightweight).^[1–10] The rational design of conducting polymers has been a challenging subject from both experimental^[11] and theoretical^[12] sides; consequently, desired properties related to the optical band gap and the redox potential (i.e., electron affinity and ionization potential) can nowadays be realized at will. In addition to the inherent functions of the polymer, the incorporation of photo- and electroactive molecules either on the side chain or backbone of the polymer leads to more advanced materials.^[13–36] For example, a donor/acceptor couple or p–n heterojunction facilitates the conversions of excitons into electrons and holes or vice versa in the material, which is applicable to photovoltaics and electroluminescence devices. In addition, when these two components are conjugated in such a way that some chemical stimuli (i.e., analytes) can perturb the

electronic interactions between them, the integrated materials function as chemosensors.^[37,38] Thus, conducting polymers functionalized with photo- and electroactive molecules, mostly π -conjugated molecules, such as porphyrins,^[14–19] phthalocyanines,^[20,21] perylenes,^[22–25] fullerenes,^[26–28] and so forth,^[29–36] have been reported. A recent example reported by Würthner and co-workers showed that oligothiophene-functionalized perylene bis(imide)s yield polymeric networks that consist of alternating p- and n-type materials at the molecular level.^[22,23] Swager and co-workers reported that a porphyrin-incorporated polythiophene network structure acts as a highly sensitive conductometric fluoride ion sensor.^[17] In these functionalized polymeric materials, not only the control of the electronic interaction between the polymer backbone and the incorporated functional molecule but also the prevention of self-aggregation of these π -conjugated systems is of importance. For instance, a charge-transfer interaction between these two components at the ground state often limits efficient charge transport. In addition, self-aggregation may cause deactivation processes of the excited state (i.e., self-quenching), such as the coupling of excitations, excimer formation, and so forth.^[39–45] Therefore, in practice, there is often a tradeoff in the incorporation of functional molecules into conducting polymers: spatial isolation of the functional molecules in the materials and yet a desired electronic interaction with the polymer backbone are required.

In this context, we herein present a new concept in monomer design toward dye-functionalized polymeric materials. We have succeeded in the syntheses of bithiophene-functionalized doubly strapped porphyrin derivatives as electro-

[a] Dr. K. Sugiyasu, Dr. M. Takeuchi
Macromolecules Group, Organic Nanomaterials Center
National Institute for Materials Science, 1-2-1 Sengen
Tsukuba, 305-0047 (Japan)
Fax: (+81)29-859-2101
E-mail: Sugiyasu.Kazunori@nims.go.jp
Takeuchi.Masayuki@nims.go.jp

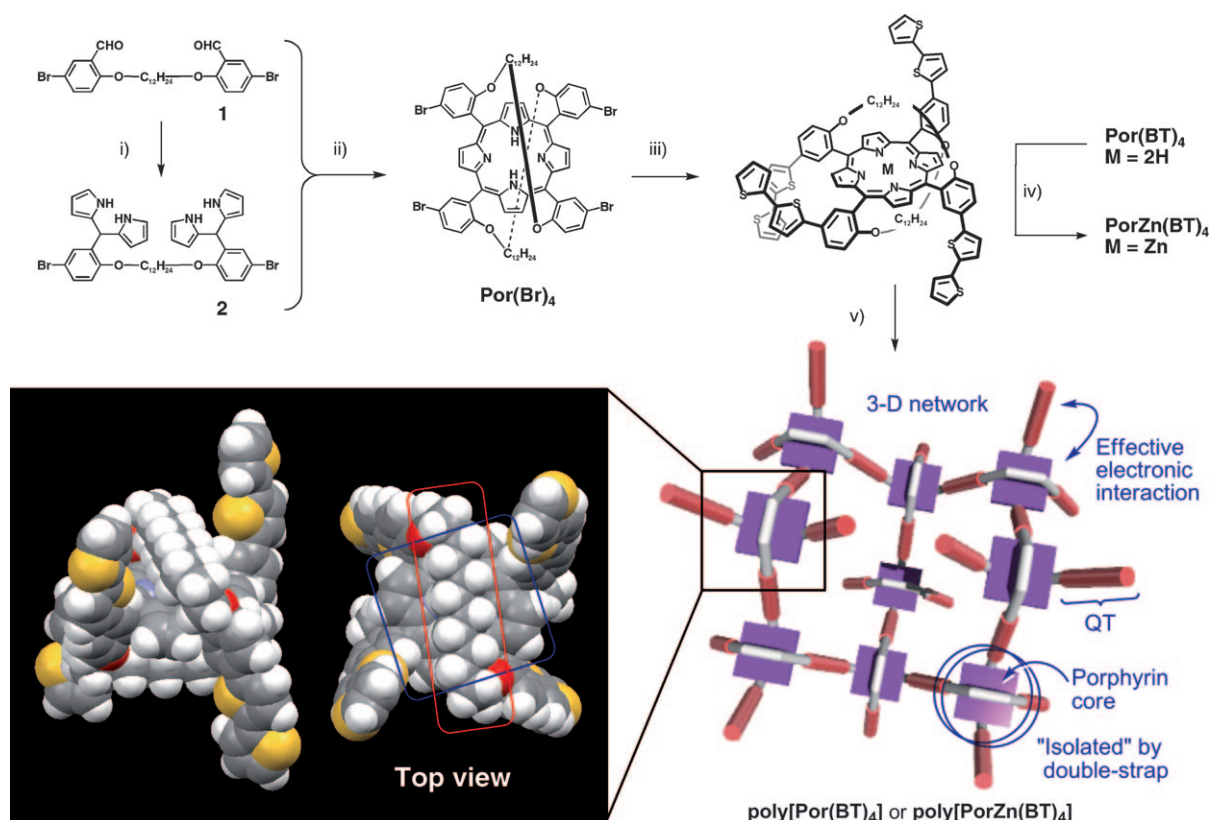
Supporting information for this article is available on the WWW under <http://dx.doi.org/10.1002/chem.200900576>.

chemically polymerizable monomers. The “double strap” is expected to shield the large π -conjugated system of the porphyrin molecule to suppress self-aggregation. Porphyrin chromophores have been extensively used as photonic and electronic materials for a long time, originally inspired by the natural photosynthetic reaction center. A large molar absorptivity in the visible region and moderate redox potentials are attractive features for optoelectronic devices.^[46–48] Furthermore, porphyrin molecules can be a good probe to demonstrate the “isolation” effect because the self-aggregation phenomena of porphyrin derivatives have been studied in detail by means of spectroscopic methods.^[49] In addition, a metal insertion reaction into the porphyrin core will indirectly show how sterically crowded the porphyrin surface is. On the other hand, oligothiophenes are known as a p-type charge carrier and can easily be polymerized by an electrochemical oxidative coupling reaction, which is a straightforward method to obtain modified electrodes. In fact, intriguing supramolecular combinations of these two building blocks have been reported so far;^[50–52] nevertheless, the design and application of the corresponding polymeric materials are still limited. Electrochemical polymerization of the present monomers based on the doubly strapped porphyrin will yield conducting polymer networks in which functional

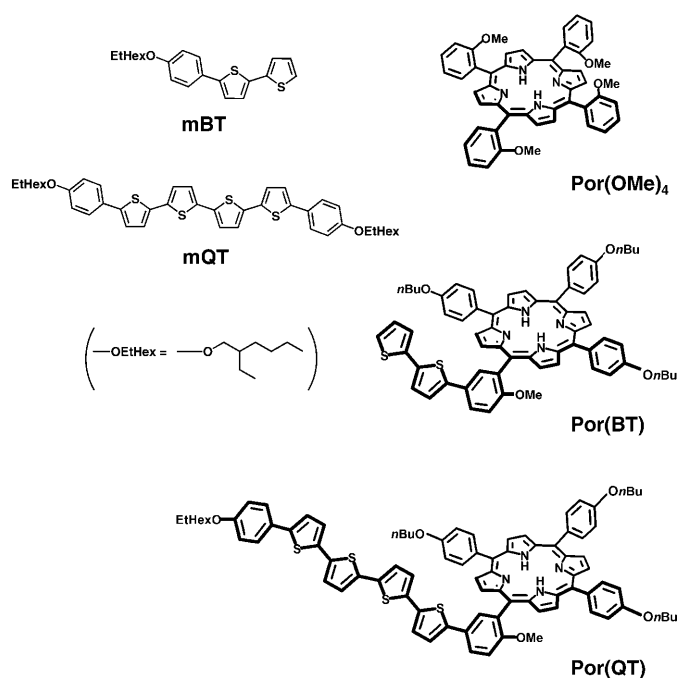
molecules (i.e., porphyrins in this study) are spatially incorporated and isolated and yet show an effective electronic interaction with the polymer backbone (see below). Herein, a basic concept of molecular design, synthesis, and characterization of porphyrin/bithiophene monomers and their photo-physical and electrochemical characteristics are described.

Results and Discussion

Synthesis of the monomer and its model compounds: The structures of electrochemically polymerizable porphyrin/bithiophene monomers (i.e., **Por(BT)₄** and **PorZn(BT)₄**) and their model components (i.e., **mBT**, **mQT**, **Por(OMe)₄**, **Por(BT)**, and **Por(QT)**) are shown in Schemes 1 and 2 (hereafter, **BT** and **QT** denote the bithiophene segments in **Por(BT)₄**, **PorZn(BT)₄**, or **Por(BT)** and quaterthiophene segments in **poly[Por(BT)₄]**, **poly[PorZn(BT)₄]**, or **Por(QT)**, respectively). **Por(QT)** has a **QT** segment on a porphyrin scaffold and was synthesized as a soluble model compound for the **poly[Por(BT)₄]** network structure, which is obtained by an electrochemical coupling reaction among the **BT** segments in **Por(BT)₄**.



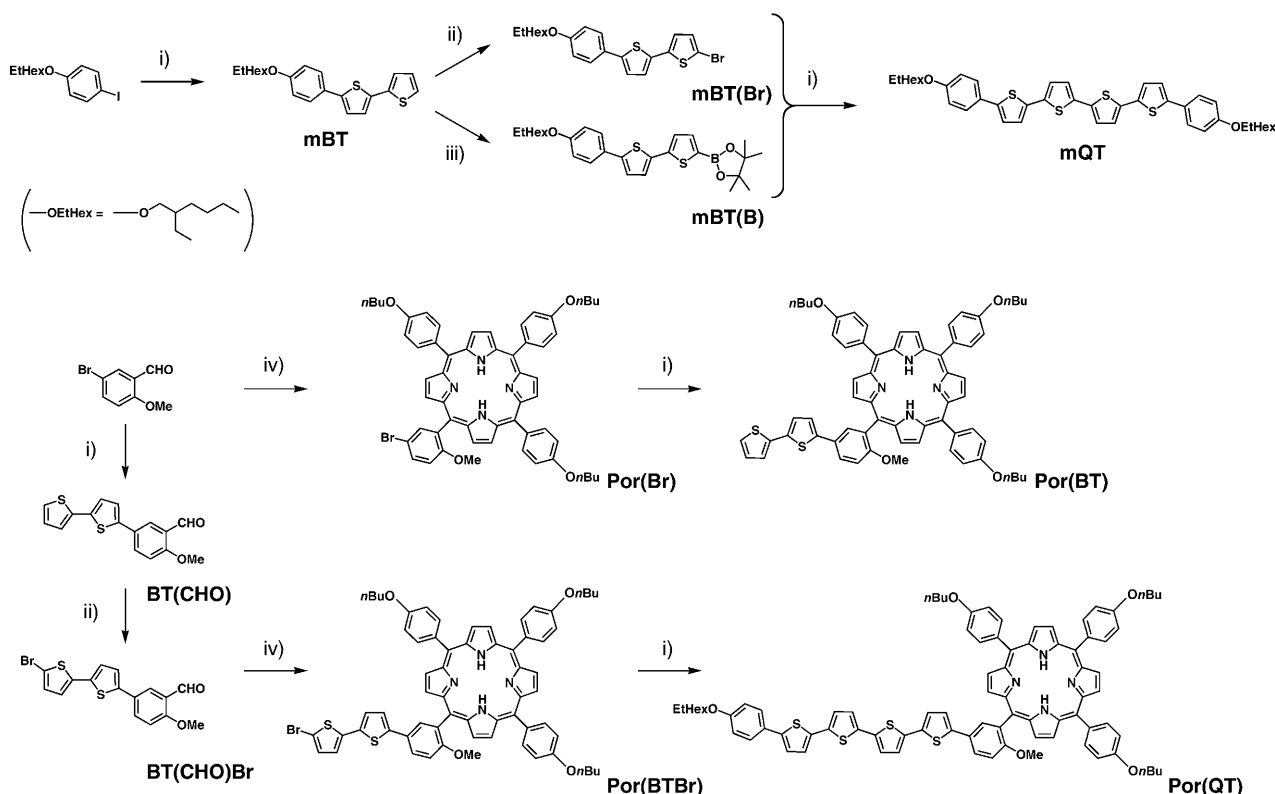
Scheme 1. Syntheses and chemical structures of doubly strapped porphyrin/bithiophene monomers **Por(BT)₄** and **PorZn(BT)₄**. Reagents and conditions: i) pyrrole, TFA; ii) $\text{BF}_3 \cdot \text{Et}_2\text{O}$, then chloranil; iii) Suzuki–Miyaura coupling reaction using $[\text{Pd}(\text{PPh}_3)_4]$ and Na_2CO_3 ; iv) zinc acetate; and v) electrochemical polymerization. A schematic representation of the polymeric network structure is shown. Purple square = porphyrin, red rod = quaterthiophene, and gray bar = alkyl chain strap. Left) Computer-generated model of **Por(BT)₄**, in which the red and blue enclosures indicate the alkyl chain strap and porphyrin surface, respectively. Right) Structure of the three-dimensional network. TFA = trifluoroacetic acid.



Scheme 2. Chemical structures of the model components: **mBT**, **mQT**, **Por(OMe)₄**, **Por(BT)**, and **Por(QT)**.

The syntheses of **mBT** and **mQT** were carried out by previously reported well-established thiophene chemistry, and the resulting molecules were characterized by using the usual methods. **Por(OMe)₄** was synthesized according to a reported procedure^[53] and purified by column chromatography (silica gel, hexane/chloroform = 4:1–0:1). The ¹H NMR spectrum of **Por(OMe)₄** at room temperature showed multiple resonances, however, each integral was identical to a tetrakis(2-substituted phenyl)porphyrin: 8H for the β position of the pyrrole unit, four sets of 4H for the 2-methoxyphenyl groups, 12H for the methoxy groups, 2H for the inner protons, and no other ambiguous peaks were observed. With two-dimensional TLC analysis, the product gave two main spots and one faint spot along the *x* axis. After heating the TLC plate at 80°C for 30 min, each spot separated into three spots on the *y* axis. These results indicate that the obtained **Por(OMe)₄** is pure but a mixture of atropisomers, as reported previously.^[53] In fact, these atropisomers are known to isomerize at a slower rate than the ¹H NMR time scale but not slow enough to be isolable.^[53]

The synthesis of the doubly strapped porphyrin intermediate **Por(Br)₄** is shown in Scheme 1 (see the Experimental Section). We have developed a new synthetic approach toward *meso*-phenyl doubly strapped porphyrin derivatives from the bis(formylphenyl) and bis(dipyrrolylmethylphenyl) straps (**1** and **2**, respectively) under Lindsey conditions,^[54,55] which selectively yield the distal (5,15:10,20)-strapped de-



Scheme 3. Syntheses and chemical structures of the model components. Reagents and conditions: i) Suzuki–Miyaura coupling using [Pd(PPh₃)₄], Na₂CO₃, and the corresponding boronic acid; ii) NBS; iii) *n*BuLi, then 2-isopropoxy-4,4,5,5-tetramethyl-1,3,2-dioxaborolane; iv) pyrrole, propionic acid. NBS = *N*-bromosuccinimide.

sired porphyrin over the proximal (5,20:10,15)-strapped by-product in a moderate yield (ca. 25%; for **Por(Br)₄**: $R_f = 0.25$, chloroform/hexane = 1:2). It is convenient that no other porphyrin derivatives were observed by TLC analysis, thus indicating that “scrambling” of pyrrole units does not take place under these reaction conditions.^[55] It should be noted that most synthetic methodologies, that is, porphyrin synthesis followed by strapping two sets out of four phenyl groups, can yield a proximal strapped porphyrin that may have $\alpha,\alpha,\alpha,\alpha$ and $\alpha,\alpha,\beta,\beta$ stereoisomers, which causes poor yield on isolation.^[56–58] In addition, another synthetic attempt starting from **1** with two equivalents of pyrrole did not give **Por(Br)₄**, instead we obtained some porphyrin derivatives, of which the ¹H NMR spectrum was complicated probably due to the aforementioned isomers (see Figure S1 in the Supporting Information for the ¹H NMR and absorption spectra; $R_f = 0.18$, chloroform/hexane = 1:2, MALDI-TOF-MS: observed m/z : 1327.74 [$M+H^+$], the same as that of **Por(Br)₄**).

The electrochemically polymerizable porphyrin/bithiophene monomer **Por(BT)₄** was synthesized from **Por(Br)₄** by using the Suzuki–Miyaura coupling reaction with 2,2'-bithiophene-5-boronic acid pinacol ester in a moderate yield (46%). The Stille coupling reaction from **Por(Br)₄** with 5-tributylstannyl-2,2'-bithiophene ([Pd(PPh₃)₄], DMF) was also applicable but resulted in a lower yield (approximately 20%). For another monomer **PorZn(BT)₄**, the zinc insertion reaction was conducted over four days (at 70°C), which is quite a long reaction time relative to that for common porphyrins (see below). Four bithiophene segments that diverge from the porphyrin core yield a polymeric network through an oxidative coupling reaction (**poly[Por(BT)₄]** or **poly[PorZn(BT)₄]**). Alkyl chain straps on each face of the porphyrin molecule are expected to shield a large π surface; as can be seen from the computer generated model of **Por(BT)₄** (Scheme 1), about 50% of the porphyrin surface is indeed concealed. Furthermore, rotational fixation of the *meso*-phenyl groups by the double straps will define the polymerization direction, which would result in a three-dimensionally cross-linked structure.^[36] A *meta*-phenylene linkage of the oligothiophene segments to the porphyrin core will suppress electronic conjugation between them,^[59] which would allow the consideration that there is a negligible ground-state interaction between the **BT** segments and porphyrin molecule. **Por(BT)** and **Por(QT)** were synthesized from 2-methoxy-5-bromobenzaldehyde or 2-methoxy-5-(5'-bromo-2,2'-bithien-5-yl)benzaldehyde, respectively, with 4-butoxybenzaldehyde and pyrrole under the Adler conditions. It is noteworthy that in the synthesis of **Por(BT)** and **Por(QT)** we planned the porphyrin synthesis in the penultimate step because the Adler condition employed two aldehyde starting materials, which potentially yields six different kinds of porphyrins that are difficult to separate. Porphyrin derivatives with one bromo reaction site (see the Experimental Section and Scheme 3 for **Por(Br)** and **Por(BTBr)**) were isolated by column chromatography (silica gel, dichloromethane/acetone/hexane = 2:1:8, twice) as second

component followed by tetrakis(4-butoxyphenyl)porphyrin. These monobrominated porphyrin derivatives were further subjected to the Suzuki–Miyaura coupling reaction with the corresponding thiophene boronic acids. Consequently, model porphyrin compounds (i.e., **Por(BT)** and **Por(QT)**) that were pure enough for spectroscopic studies were synthesized.

Characterization of the “double strap”: The ¹H NMR spectrum of **Por(Br)₄** showed a singlet peak for the β proton of pyrrole ($\delta = 8.77$ ppm) in clear contrast to those peaks of **Por(OMe)₄**, thus indicating a symmetric structure (see the Supporting Information). In addition, alkyl chain straps appeared in the upfield region ($\delta = -0.13$ – 0.89 ppm) due to the strong ring-current effect of the porphyrin molecule (see Figure S2 in the Supporting Information). This result demonstrates that the alkyl chain straps are lying in the porphy-

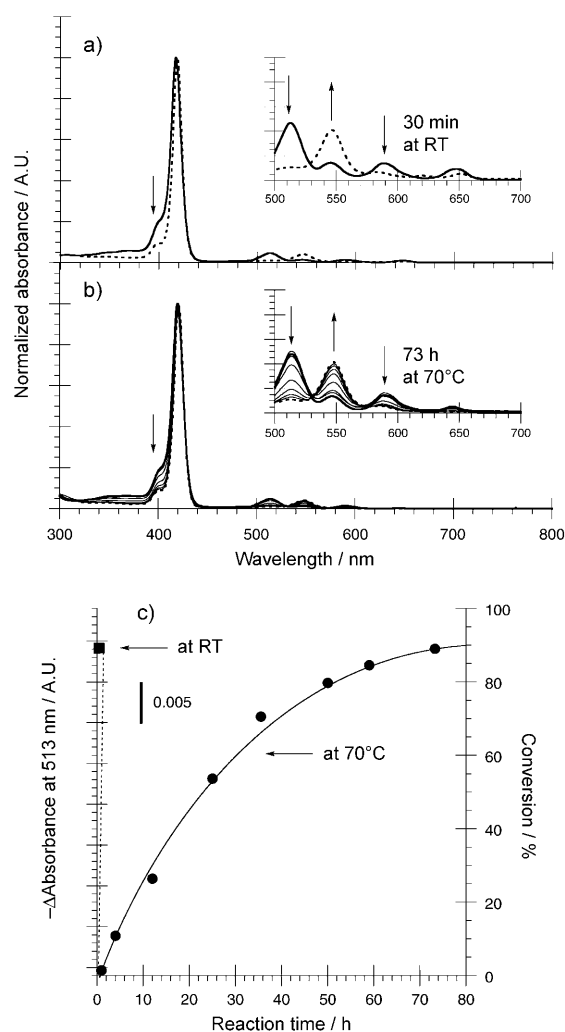


Figure 1. Absorption spectral changes of a) **Por(OMe)₄** and b) **Por(Br)₄** measured during the zinc insertion reaction: dotted lines are the spectra measured after the reaction was completed. c) Plots of the absorption intensity change at $\lambda = 513$ nm as a function of the reaction time: **Por(OMe)₄** at RT (squares) and **Por(Br)₄** at 70°C (circles). The reaction conversions were determined by using the ¹H NMR spectroscopic data shown in Figure 2.

rin plane. Another evidence of the shielded porphyrin was obtained by monitoring a zinc insertion reaction. In general, this reaction is completed within 30 min at room temperature; for example, the absorption spectral change of **Por(OMe)₄** on the addition of zinc acetate is shown in Figure 1 a. The observed spectral change is consistent with that observed through zinc complexation. In contrast, in the case of **Por(Br)₄**, we needed to heat up the reaction mixture to see the same spectral changes (Figure 1 b). Figure 2 shows the ¹H NMR spectral changes of **Por(Br)₄** measured during the zinc insertion reaction. After a reaction time of 25 h (at

70 °C, see the Experimental Section for details), a new set of peaks assignable to a porphyrin derivative was observed together with the starting material (conversion = 53 %). A sharper peak for a new β-pyrrole proton relative to the spectrum of **Por(Br)₄** arises from the conformational fixation of the porphyrin plane by the zinc complexation. Plots of the changes in absorption intensity as a function of the reaction time is shown with the reaction conversions determined by the ¹H NMR spectroscopic data (Figure 1 c). It took three days at 70 °C for > 90 % of **Por(Br)₄** to be converted into the zinc complex (MALDI-TOF-MS: *m/z*: 1389.7

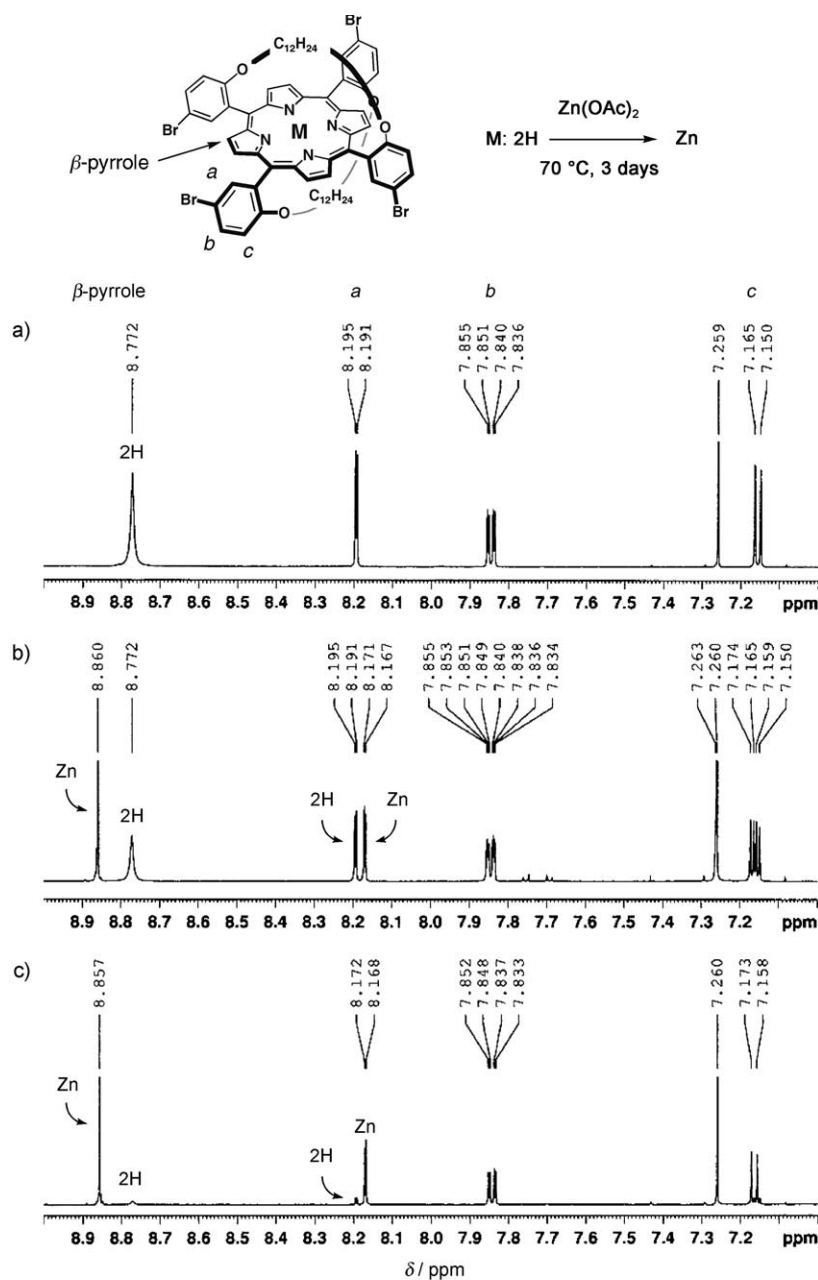


Figure 2. ¹H NMR spectra of **Por(Br)₄** measured during the zinc insertion reaction after the reaction time of a) 1, b) 25, and c) 73 h.

[**PorZn(Br)₄+H⁺**]; calcd: 1389.1). It should be noted here that the 1,12-dodecyl strap is long enough not to curve the porphyrin plane,^[60] and is thus ineffective toward the stability of the metal complex in respect of the thermodynamic factor. These results clearly show that both faces of the porphyrin molecule are overlaid with the bulky alkyl chain straps.

Spectroscopic measurements of solid films: The isolation of photofunctional molecules, thus evidenced, should affect the photophysical properties, particularly in the solid phase. To probe this “isolation effect”, we measured the absorption spectra of **Por(OMe)₄**, **Por(Br)₄**, and **Por(BT)₄** in the film states (prepared on a glass plate by spin-coating; Figure 3). In the film states, the absorption maxima of these porphyrin derivatives were red-shifted in comparison with those measured in dilute solutions of dichloromethane (1×10^{-6} M): $\Delta\lambda = 17.5$, 12.5, and 10.5 nm for **Por(OMe)₄**, **Por(Br)₄**, and **Por(BT)₄**, respectively, namely smaller shifts with the double straps. In addition, the average full width at half maximum (FWHM) of the Soret band of **Por(Br)₄** (163 meV) was smaller than that of **Por(OMe)₄** (228 meV); however, the FWHM of **Por(BT)₄** (203 meV) was slightly larger than expected, which is due to the absorption overlap of the bithiophene groups with the Soret band of the porphyrin (see Table 1 for the data on

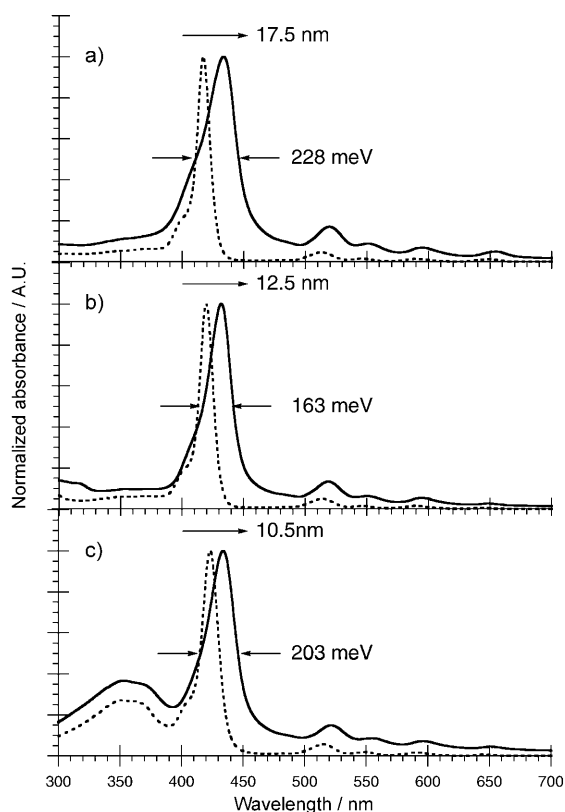


Figure 3. Absorption spectra of the spin-coated films (solid line) and dilute solutions (dotted line) of a) **Por(OMe)₄**, b) **Por(Br)₄**, and c) **Por(BT)₄**.

Table 1. Absorption spectroscopic data of the porphyrin derivatives.^[a]

Compound	λ_{\max} in solution [nm]	λ_{\max} in film [nm]	$\Delta\lambda_{\max}$ [nm]	FWHM in film [meV]
Por(OMe)₄	417.0	434.5	17.5	228
Por(BT)₄	422.0	438.0	16.0	228
Por(QT)	422.0	437.0	15.0	n.d. ^[b]
Por(Br)₄	419.5	432.0	12.5	163
Por(BT)₄	423.5	434.0	10.5	203
PorZn(BT)₄	425.0	438.0	13.0	193

[a] Determined for the Soret bands of the porphyrin. [b] Not determined because of the significant overlap between the Soret band of the porphyrin and the absorption of the **QT** segment.

other porphyrin derivatives). These results indicate that in the solid films, the double strap prevents the porphyrin molecule from self-aggregation. Consequently, the fluorescence of the **Por(BT)₄** films was about twice as strong as that of **Por(OMe)₄** ($\lambda_{\text{ex}} = 440$ nm; Figure 4). Note that the fluorescence intensities were normalized by the optical densities of each film at the excitation wavelength. The improvement in photoluminescent efficiency in the solid phase is comparable with that confirmed for cyclodextrin-threaded conjugated polyrotaxanes, “insulated conjugated polymers”, which shows better electroluminescence efficiency than bare conjugated polymers.^[61] We expect that not only the shielding around the π plane of the porphyrin but also the three-dimensional persistent structure, both of which are conferred

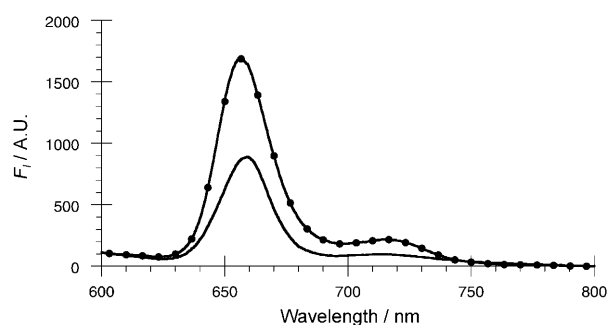


Figure 4. Fluorescence spectra of the spin-coated films of **Por(OMe)₄** (solid line) and **Por(BT)₄** (solid line with filled circle; $\lambda_{\text{ex}} = 440$ nm). Note that the fluorescence intensities are normalized by the optical densities of each film at the excitation wavelength.

by the alkyl chain straps, prevent the porphyrin molecules from aggregation, thus significant fluorescence can be achieved even in the solid phase.

Light-harvesting studies: To elucidate an electronic interaction between the oligothiophene segments and the porphyrin core, the light-harvesting ability of **Por(BT)₄** was investigated in a dilute solution of dichloromethane (1×10^{-6} M). We measured the UV/Vis absorption and steady-state fluorescence spectra of the **Por(BT)₄** monomer and its model components (Figures 5 and 6 a, respectively). The absorption band around $\lambda = 350$ nm observed for **Por(BT)₄** is attributed to the **BT** segments: a margin of molar absorptivities at this wavelength between **Por(BT)₄** and **Por(OMe)₄** is about fourfold larger than the molar absorptivity of **mBT**, thus indicating a fourfold bithiophene-functionalization. Furthermore, no additional distinctive absorption bands attributable to a charge-transfer complex are observed, which is indicative of an insignificant ground-state electronic interaction between these two chromophores in **Por(BT)₄**. Relative fluorescence quantum yields Φ_{F} of these compounds were determined against rhodamine B ($\Phi_{\text{F}} = 0.97$ in ethanol) for porphyrin derivatives and quaterthiophene ($\Phi_{\text{F}} = 0.18$ in benzene^[62]) for **mBT** and **mQT** as standards: $\Phi_{\text{F}} = 0.023, 0.023, 0.095,$ and 0.25 for **Por(OMe)₄**, **Por(BT)₄**, **mBT**, and **mQT**, respectively. When **Por(BT)₄** was photoexcited at a wavelength ($\lambda = 350$ nm) at which selective excitation for the **BT** segments is possible, the fluorescence from the bithiophene units was completely quenched ($>99\%$ decrease relative to a pure solution of **mBT**; Figure 6 a). In addition, the fluorescence of the porphyrin was intensified by fivefold in comparison with the fluorescence from **Por(OMe)₄** ($\lambda_{\text{ex}} = 350$ nm; Figure 6 a inset). These results indicate that efficient energy transfer from the bithiophene segments to the porphyrin molecule takes place in the **Por(BT)₄** system. The excitation spectra of **Por(BT)₄** and **Por(OMe)₄** monitored at $\lambda = 650$ nm further demonstrated the contribution of **BT** to the fluorescence of porphyrin (Figure 6 b). The same light-harvesting phenomenon was also observed for the **PorZn(BT)₄** system (see Figure S3 in the Supporting Information). In fact, the fluorescence spectrum of **mBT** ($\lambda_{\text{ex}} = 400\text{--}450$ nm) overlaps well with the Soret absorption band

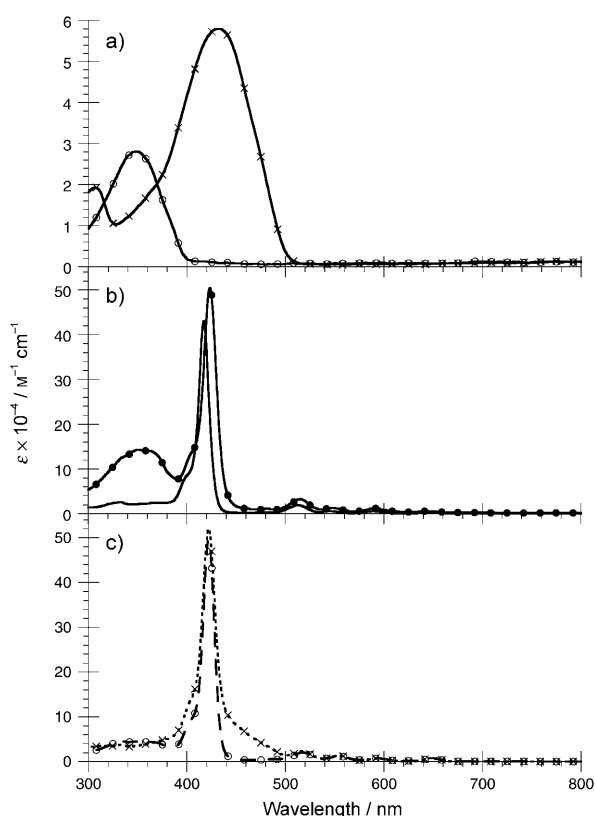


Figure 5. Absorption spectra of a) **mBT** (solid line with open circle) and **mQT** (solid line with cross), b) **Por(OMe)₄** (solid line) and **Por(BT)₄** (solid line with filled circle), and c) **Por(BT)** (dash-dot line with open circle) and **Por(QT)** (dotted line with cross) in a dilute solution of dichloromethane (1×10^{-6} M).

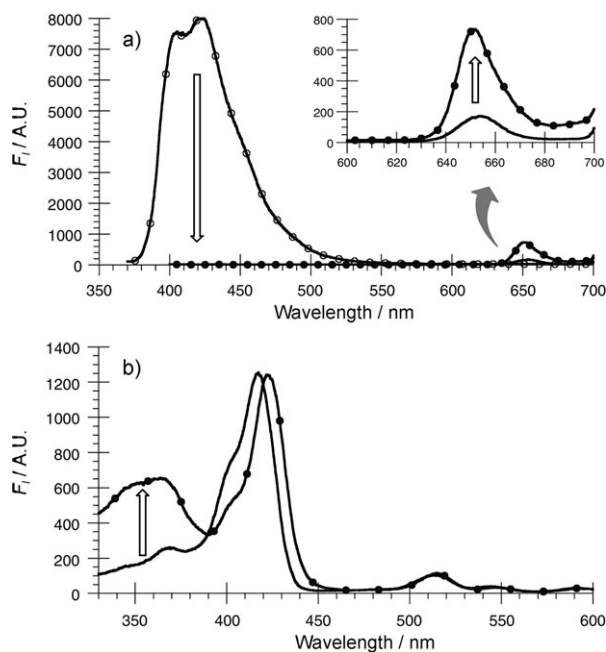


Figure 6. a) Fluorescence and b) excitation spectra of **Por(OMe)₄** (solid line), **Por(BT)₄** (solid line with filled circle), and **mBT** (solid line with open circle) in a dilute solution of dichloromethane. Inset shows magnified fluorescence spectra: $[\text{Por(OMe)}_4] = [\text{Por(BT)}_4] = 1 \times 10^{-6}$ M; $[\text{mBT}] = 4 \times 10^{-6}$ M; $\lambda_{\text{ex}} = 350$ nm, $\lambda_{\text{mon}} = 650$ nm; RT.

of the porphyrin molecules. Furthermore, this light-harvesting effect was confirmed with a spin-coated film of **Por(BT)₄**; a quantitative quenching of the fluorescence of **BT** segments and an enhanced fluorescence of porphyrin by about 5.2-fold were observed ($\lambda_{\text{ex}} = 350$ nm; see Figure S4 in the Supporting Information). As mentioned earlier (Figure 4), a photoluminescence improvement of about two-fold in the solid phase (versus **Por(OMe)₄**, $\lambda_{\text{ex}} = 440$ nm) is indebted to the isolation by the double strap, therefore, an increase of approximately 260% out of 520% would roughly be attributed to the light-harvesting effect in the film state.

To prospect the light-harvesting ability of the **poly-[Por(BT)₄]** film, the fluorescence and excitation spectra of **Por(QT)** and **Por(BT)** ($\Phi_{\text{F}} = 0.036$ and 0.035 , respectively) were also measured. Although the spectral overlaps between the fluorescence of the donors (i.e., **BT** or **QT**) and the absorption of porphyrin are different, both systems showed quantitative energy transfer (see Figures S5 and S6 in the Supporting Information). For example, selective excitation of the **QT** segment in **Por(QT)** resulted in no fluorescence from **QT** but yielded an enhanced fluorescence by 27-fold from the porphyrin core relative to that of **Por(OMe)₄** ($\lambda_{\text{ex}} = 440$ nm). In fact, the excitation spectrum of **Por(QT)** revealed a significant contribution of the absorption by **QT** to the fluorescence from porphyrin (this finding can obviously be evidenced by the broad range of excitation at $\lambda = 440 \sim 490$ nm, although the absorption peaks of porphyrin and **QT** are partially overlapping; see Figure S6b in the Supporting Information). Considering that the fluorescence quantum yield of **Por(QT)** is almost the same as that of **Por(BT)**, additional quenching by the contribution of electron transfer (i.e., a nonradiative process) between **QT** and the porphyrin core is negligible relative to **Por(BT)**, regardless of the difference in the relative HOMO–LUMO energies of **BT** and **QT** with respect to those of porphyrin molecule.^[15,22] These results indicate that our molecular design of the energy donor–acceptor conjunction, such as the distance between these two components and the orientation of their transition dipole, is appropriate.

Electrochemical polymerization and characterization: Cyclic voltammograms of **Por(BT)₄** and **PorZn(BT)₄** were measured in an argon atmosphere with 100 mM tetrabutylammonium hexafluorophosphate (TBAPF₆) in dichloromethane ($[\text{monomer}] = 0.5$ mM). When the oxidation potential was swept up to 0.56 V (versus the ferrocene/ferrocenium redox couple (Fc/Fc⁺)), reversible redox waves of each porphyrin molecule were observed at $E_{1/2} = 0.46$ and 0.39 V for **Por(BT)₄** and **PorZn(BT)₄**, respectively (Figure 7a,c). This result implies that the redox potentials of the incorporated dyes can easily be controlled by metal complexation, which will enable fine-tuning of the electronic properties of the materials. Further repeated potential sweeps between -0.01 and 0.69 V gradually yielded quasi-reversible redox waves (Figure 7b,d), thus indicating electrochemical polymerization processes. The growth of the polymer network is reflected by a proportional increase in the current to the po-

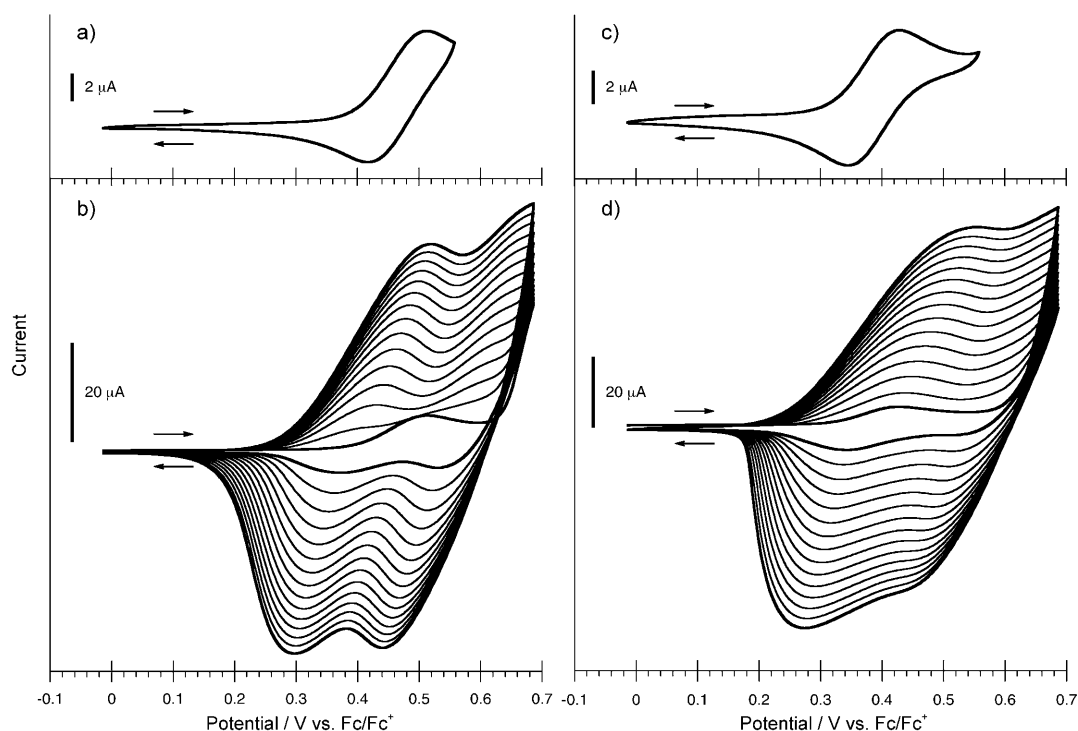


Figure 7. Cyclic voltammograms of **Por(BT)₄** and **PorZn(BT)₄** measured up to a,c) 0.56 and b,d) 0.69 V (15 scans). [monomers]=0.5 mM, [TBAPF₄]=100 mM, dichloromethane, 100 mV s⁻¹, RT.

tential cycles. New redox waves at around $E_{1/2}^1=0.40$ V and $E_{1/2}^2=0.55$ V correspond to the constructed **QT/QT⁺** and **QT⁺/QT²⁺** redox couples, respectively, accompanied with the superimposed redox processes of the porphyrin; note that redox potentials of the components (i.e., **BT**, **QT**, and porphyrin) can affect each other in the film as demonstrated by the cyclic voltammogram of **Por(QT)** (see Figure S7 in the Supporting Information), therefore the cyclic voltammograms of these films become somewhat structureless.

The obtained **poly[Por(BT)₄]** and **poly[ZnPor(BT)₄]** films were electrochemically characterized in an electrolyte solution free from the monomer. The linear scan-rate dependences of these films demonstrate that the redox process originates from electrode-bound redox-active species (Figure 8a,b,d,e). The films were uniform and adhesive to the working electrode, probably due to the highly cross-linked network structure. Differential potential voltammetry (DPV) of the obtained films gave evidence of the incorporation of the porphyrin molecule. Although the oxidation peaks of the incorporated porphyrins (Figure 7a,c and Figure 8c,f; solid line) were concealed beneath those of the constructed **QT** segments, the reduction peaks of which were observable in DPV as also observed for the monomer solution at around -2 V (Figure 8c,f; dotted line). A molar ratio of 4:1 between the bithiophene segments and the porphyrin core in the monomers can ideally yield polymeric network films composed of the constructed **QT** segments and the porphyrin in a 2:1 ratio. However, the area of the oxidation peak of the films relative to the reduction peak of the porphyrin was slightly smaller than this expected ratio

(**QT**/porphyrin=1.6:1). This result indicates that there are starting material bithiophene defects that can still function as the energy donor in the network structure. The absorption spectrum of the **poly[Por(BT)₄]** film deposited on an indium tin oxide (ITO)-coated glass electrode indeed evidenced the existence of the **BT** ($\lambda=320\text{--}380$ nm) and constructed **QT** ($\lambda=360\text{--}480$ nm) segments (Figure 9). Moreover, the four characteristic Q bands at $\lambda=517, 550, 590,$ and 645 nm are identical to those of free base porphyrin (no peak shift relative to those of the **Por(BT)₄** spin-coated film). These results indicate that the porphyrin molecule is "isolated" as demonstrated with the spin-coated films of the monomer without any decomposition or protonation (see Figure S8 in the Supporting Information for the absorption spectrum of the **poly[PorZn(BT)₄]** film that shows a Q band at $\lambda=556$ nm, which is identical to that of the **PorZn(BT)₄** film). It should be noteworthy that electrochemical polymerization of bithiophene-functionalized metal-free porphyrins is in most cases unsuccessful due to the interference of the porphyrin nitrogen atoms with the oligothiophene radical cations.^[18] It seems that the double strap could also play an important role in protecting the porphyrin molecule against the electrochemical polymerization conditions. As proved from the model studies mentioned earlier, the polymeric films can harvest a wide range of irradiation light ($\lambda=320\text{--}650$ nm) into the porphyrin core and suppress undesired deactivation processes. However, the electrochemically polymerized films were nevertheless nonfluorescent. One main reason for this behavior should be that porphyrin molecules have intrinsically low fluorescence quantum yields. Other

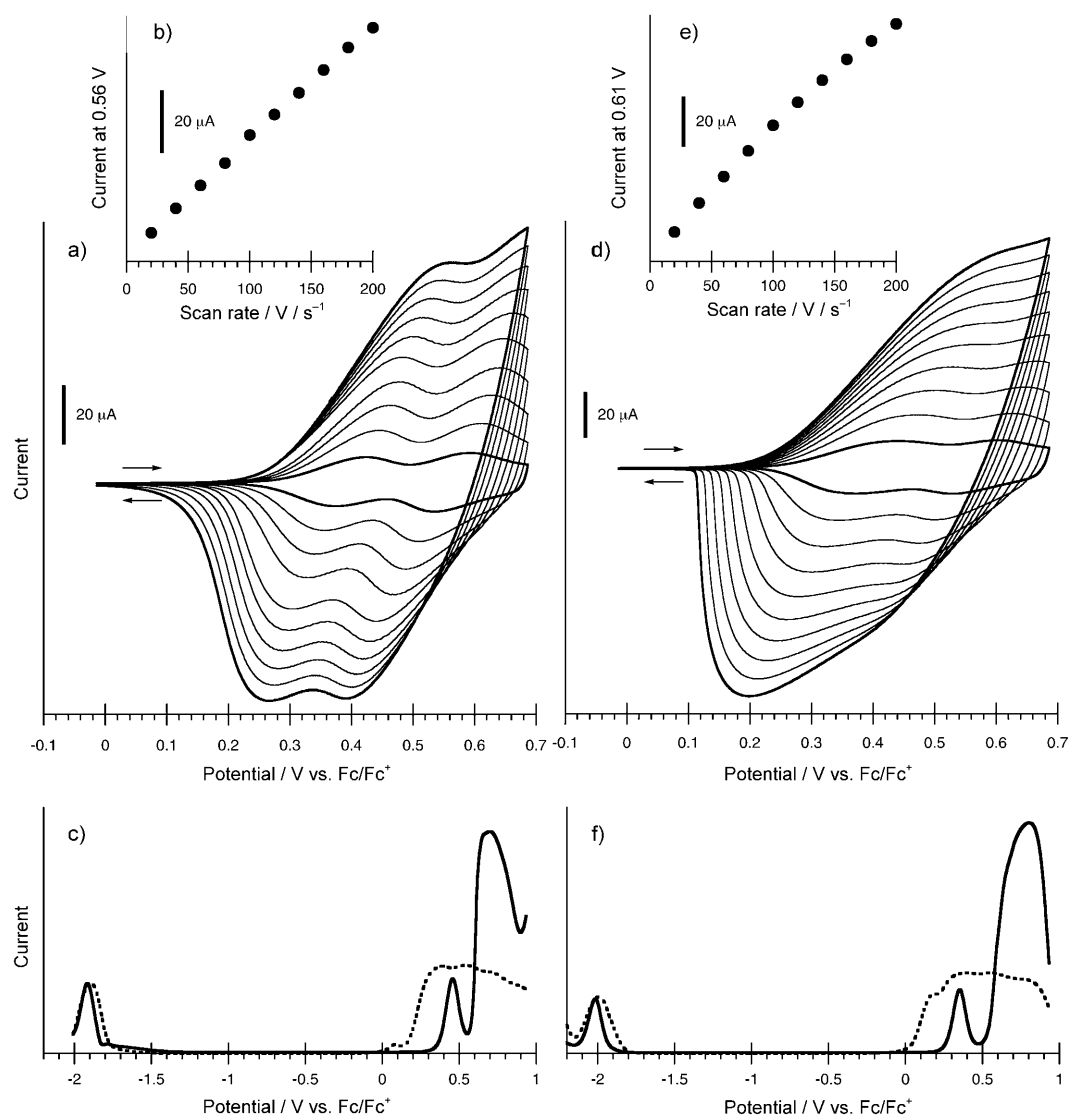


Figure 8. Cyclic voltammograms of the a) **poly[Por(BT)₄]** and d) **poly[PorZn(BT)₄]** films measured with different scan rates: 20, 40, 60, 80, 100, 120, 140, 160, and 200 mVs^{-1} from inwards to outwards. Plots of the observed current as a function of the scan rate for the b) **poly[Por(BT)₄]** and d) **poly[PorZn(BT)₄]** films. DPVs of the monomers in solution (solid line) and the corresponding polymer films (dotted line) for the c) **Por(BT)₄** and f) **PorZn(BT)₄** systems.

possible reasons for the fluorescence quenching factors, such as the effect of the band structure of the ITO electrode (see Figure S9 in the Supporting Information), the electrolyte used, and the presence of a trace amount of oxidized species, would also need to be considered. We will therefore focus on the development of our strategy by making use of other functional dyes and the detailed optimization of the electrochemical polymerization conditions.

Conclusions

Herein, a new concept in monomer design toward dye-functionalized conducting polymeric materials has been described. The main strategies of our monomer design are 1) the functional dyes are spatially isolated within the poly-

meric material by the double strap, which can prevent the large π -conjugated system from self-aggregation; 2) the conjugations composed of functional dyes and conducting polymer backbones are designed in such a way that there is an effective electronic interaction between them in spite of the "isolation" of the incorporated dyes. These two distinctive features were evidenced by using $^1\text{H NMR}$, UV/Vis, and fluorescence spectroscopic methods. These results demonstrated that with our strategy, spatial isolation of the functional dyes in the materials and effective electronic interaction between the dye and the polymer backbones can both be achieved. Hence, the concept described herein may address the "tradeoff" that often haunts dye-functionalized conducting polymers. The photo- and electrochemical characteristics were demonstrated by utilizing two different monomers, **Por(BT)₄** and **PorZn(BT)₄**, with different redox

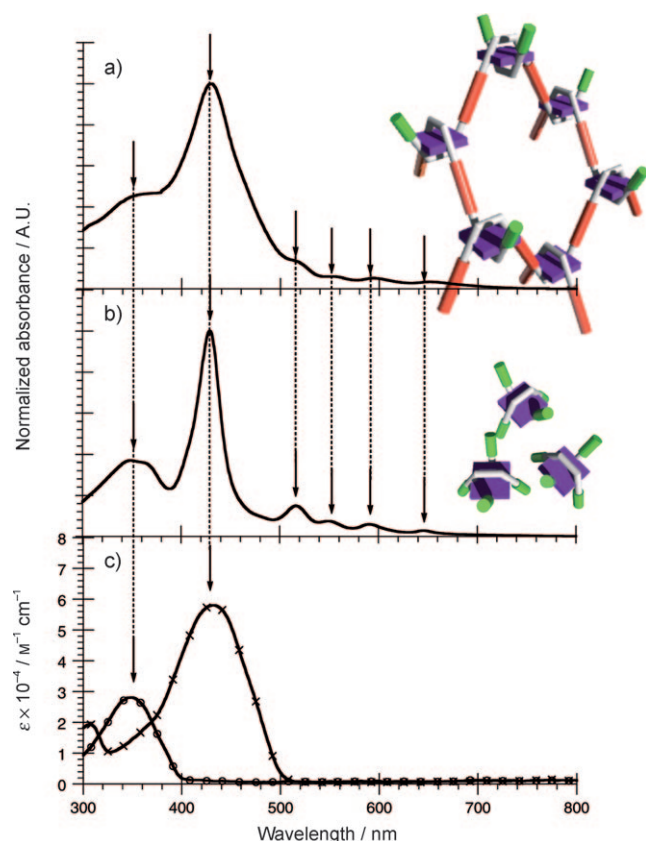


Figure 9. Absorption spectra of the a) poly[Por(BT)₄] film and b) Por(BT)₄ spin-coated film (the same as Figure 3c), and c) dilute solution of mBT (solid line with open circle) and mQT (solid line with cross) in dichloromethane (the same as the parts of Figure 5). In the schematic representation (inset cartoons), purple square = porphyrin, red rod = QT segment, green rod = BT segment, and gray bar = alkyl chain strap.

potentials. At the beginning in applying these monomers, we confirmed that electrochemical polymerization of both of them is effective and gives robust films in which the porphyrin molecules are incorporated without any decomposition and protonation. This molecular design concept based on the incorporation of “isolated” functional molecules on conducting polymers is closely related to the “insulated molecular wires” that have already found unique applications in efficient electroluminescence and ultrasensitive chemosensors,^[61,63–67] thus we will progress accordingly by taking advantage of our materials.

Experimental Section

General: Air- and water-sensitive synthetic manipulations were performed in an argon atmosphere using standard Schlenk techniques. All the chemicals were purchased from Aldrich, Kanto Chemical Co., or Wako and used as received. The NMR spectra were recorded on a Bruker Biospin DRX-600 spectrometer, and all the chemical shifts are referenced to (CH₃)₄Si (TMS; $\delta = 0$ ppm for ¹H) or residual CHCl₃ ($\delta = 77$ ppm for ¹³C). The MALDI-TOF mass spectra and high-resolution (HR) LCMS-TOF mass spectra were obtained with SHIMADZU

AXIMA-CFR Plus and SHIMADZU LCMS-IT-TOF workstation, respectively. The UV/Vis absorption and fluorescence spectra were obtained on Hitachi U-2900 and Hitachi F-7000 spectrophotometers, respectively. Relative fluorescence quantum yields were determined using quaterthiophene ($\Phi_F = 0.18$ in benzene^[62]) for mBT and mQT and rhodamine B ($\Phi_F = 0.97$ in ethanol) for Por(OMe)₄, Por(BT)₄, PorZn(BT)₄, Por(BT), and Por(QT) as standards. The melting points were determined on a Yanako NP-500P micro melting-point apparatus. All the electrochemical measurements were conducted with an Eco Chemie AUTO-LAB PGSTAT12 potentiostat with a quasi-internal Ag/Ag⁺ reference electrode (Ag wire submersed in a solution of 0.01 M AgNO₃ and 0.1 M *n*Bu₄NPF₆ in MeCN). Cyclic voltammograms were recorded with a platinum button electrode or ITO-coated glass electrode as the working electrode and a platinum-coil counter electrode. Molecular modeling was performed using ChemBio3D Ultra software available from Cambridge-Soft. Model compounds were synthesized according to Scheme 3. Monomer mBT was synthesized through the Suzuki–Miyaura coupling reaction from 4-ethylhexyloxyiodobenzene and 2,2'-bithiophene-5-boronic acid pinacol ester under the same reaction conditions as for the synthesis of Por(BT)₄ (see below). Selective bromination at the α position of mBT using NBS^[68], thus yielding mBTBr, followed by lithiation and subsequent quenching with 2-isopropoxy-4,4,5,5-tetramethyl-1,3,2-dioxaborolane gave 5-(4-ethylhexyloxyphenyl)-2,2'-bithiophene-5'-boronic acid pinacol ester (mBTB).^[69] The obtained intermediates mBTB and mBTB were further coupled through the Suzuki–Miyaura coupling reaction, thus yielding mQT. Compounds BT(CHO) and BT(CHO)Br were synthesized by using the same procedure for the synthesis of mBT and mBTB, respectively, from 2-methoxy-5-bromobenzaldehyde as a starting material. For the syntheses of mono-oligothiophene-functionalized porphyrins (Scheme 3), Por(Br) and Por(BTBr) were first synthesized under the Adler conditions^[53] from 2-methoxy-5-bromobenzaldehyde and 2-methoxy-5-(5'-bromo-2,2'-bithien-5-yl)benzaldehyde (BT(CHO)Br), respectively, with 4-butoxybenzaldehyde and pyrrole. Monofunctionalized porphyrins were isolated by column chromatography (silica gel, dichloromethane/acetone/hexane = 2:1:8) to remove other byproducts, such as tetrakis(4-butoxyphenyl)porphyrin.

Synthesis of Por(BT): A mixture of Por(Br) (0.4 g, 0.43 mmol), 2,2'-bithiophene-5-boronic acid pinacol ester (0.18 g, 0.62 mmol) and sodium carbonate (0.16 g, 1.5 mmol) in toluene (30 mL), ethanol (7.5 mL), and water (7.5 mL) was bubbled with argon for 1 h. Tetrakis(triphenylphosphine)palladium(0) (10 mol% Por(Br)) was added to the solution and the mixture was heated to reflux for 5 h. After cooling, the reaction mixture was washed with water and the organic layer was dried over sodium sulfate. The solvent was evaporated and the obtained solid was purified by column chromatography (silica gel, hexane/chloroform = 1:1–0:1) to give Por(BT) as a purple powder (0.38 g, 87%). M.p. 158–159 °C; ¹H NMR (600 MHz, CDCl₃, TMS): $\delta = -2.70$ (s, 2H), 1.09–1.12 (m, 9H), 1.63–1.69 (m, 6H), 1.94–1.99 (m, 6H), 3.62 (s, 3H), 4.24–4.27 (m, 6H), 6.98 (dd, $J = 3.6, 4.2$ Hz, 1H), 7.12 (d, $J = 4.2$ Hz, 1H), 7.14 (dd, $J = 1.2, 4.2$ Hz, 1H), 7.17 (dd, $J = 1.2, 4.2$ Hz, 1H), 7.23 (d, $J = 3.6$ Hz, 1H), 7.27–7.28 (m, 6H), 7.33 (d, $J = 8.4$ Hz, 1H), 7.99 (dd, $J = 2.4, 8.4$ Hz, 1H), 8.08–8.12 (m, 6H), 8.29 (d, $J = 2.4$ Hz, 1H), 8.83 (d, $J = 6.4$ Hz, 2H), 8.86 ppm (m, 6H); UV/Vis (dichloromethane): λ_{\max} (ϵ) = 422 (5.0×10^5), 517 (2.1×10^4), 554 (1.2×10^4), 593 (7.0×10^3), 649 nm (7.0×10^3 mol⁻¹ dm³ cm⁻¹); fluorescence spectrum (dichloromethane) λ_{em} (Φ_F) = 657 nm (0.035); MALDI-TOF-MS: m/z : calcd for C₆₅H₆₀N₄O₄S₂: 1024.41; found: 1024.41.

Synthesis of Por(QT): The same procedure for the synthesis of Por(BT) was applied using mBTB and Por(BT)Br as starting materials. M.p. 227–228 °C; ¹H NMR (600 MHz, CDCl₃, TMS): $\delta = -2.70$ (s, 2H), 0.91–0.94 (m, 6H), 1.09–1.22 (m, 9H), 1.31–1.48 (m, 8H), 1.65–1.69 (m, 6H), 1.73 (m, 1H), 1.94–1.99 (m, 6H), 3.63 (s, 3H), 3.86 (dd, $J = 2.4, 5.4$ Hz, 2H), 4.24–4.27 (m, 6H), 6.90 (d, $J = 8.4$ Hz, 2H), 7.04 (m, 4H), 7.09 (d, $J = 1.2$ Hz, 2H), 7.12 (d, $J = 3.6$ Hz, 1H), 7.24 (d, $J = 3.6$ Hz, 1H), 7.27–7.29 (m, 6H), 7.34 (d, $J = 8.4$ Hz, 2H), 7.49 (d, $J = 8.4$ Hz, 2H), 7.99 (dd, $J = 2.4, 8.4$ Hz, 1H), 8.10–8.12 (m, 6H), 8.29 (d, $J = 2.4$ Hz, 1H), 8.83 (d, $J = 4.2$ Hz, 2H), 8.86 ppm (m, 6H); UV/Vis (dichloromethane): λ_{\max} (ϵ) = 422 (5.2×10^5), 517 (2.3×10^4), 554 (1.3×10^4), 593 (7.0×10^3), 649 nm (7.0×10^3 mol⁻¹ dm³ cm⁻¹); fluorescence (dichloromethane): λ_{em} (Φ_F) = 657 nm

(0.036); MALDI-TOF-MS: m/z : calcd for $C_{87}H_{84}N_4O_5S_4$: 1392.53; found: 1393.72.

Synthesis of 1: A solution of 5-bromosalicylaldehyde (30.6 g, 152 mmol) and potassium carbonate (63.0 g, 456 mmol) in DMF (300 mL) was stirred at 70 °C for 1 h, and 1,12-dibromododecane (20.0 g, 61 mmol) was added. The reaction mixture was further stirred at 70 °C for 10 h. After cooling to room temperature, the reaction mixture was diluted with dichloromethane and the insoluble materials were filtered off. The filtrate was concentrated, and the precipitate was obtained with the addition of methanol. A solution of the obtained solid in dichloromethane was washed with 0.1 M sodium hydroxide aqueous solution and dried over magnesium sulfate. The filtrate was evaporated and the obtained solid was purified by reprecipitation from dichloromethane with methanol to give **1** as a white powder (29.8 g, 86%). M.p. 96–97 °C; 1H NMR (600 MHz, $CDCl_3$, TMS): δ = 1.29–1.37 (m, 12H), 1.47 (m, 4H), 1.84 (m, 4H), 4.06 (t, J = 6.3 Hz, 4H), 6.88 (d, J = 9.0 Hz, 2H), 7.60 (dd, J = 3.0, 9.0 Hz, 2H), 7.91 (d, J = 3.0 Hz, 2H), 10.42 ppm (s, 2H); ^{13}C NMR (150 MHz, $CDCl_3$): δ = 25.97, 28.95, 29.25, 29.47, 68.95, 113.21, 114.54, 126.12, 130.79, 138.23, 160.41, 188.44 ppm; HRMS: m/z : calcd for $C_{26}H_{32}Br_2O_4Na$: 591.0547 [$M+Na$] $^+$; found: 591.0444.

Synthesis of 2: Compound **1** (16.97 g, 29.8 mmol) and pyrrole (100 g, 1.49 mol) were dissolved in dichloromethane (200 mL), the solution was purged with argon for 1 h and trifluoroacetic acid (0.34 mL, 4.47 mmol) was added. The reaction mixture was stirred at room temperature for 5 h and washed with 0.1 M aqueous solution of sodium hydroxide. The organic layer was dried over sodium sulfate and the filtrate was evaporated to remove excess pyrrole. The crude material was purified by column chromatography (silica gel, hexane/dichloromethane = 1:2–0:1, containing 1% triethylamine). The product was further purified by reprecipitation from dichloromethane with hexane to give **2** as a white powder (8.0 g, 34%). M.p. 148–150 °C; 1H NMR (600 MHz, $CDCl_3$, TMS): δ = 1.28 (m, 16H), 1.64 (m, 4H), 3.88 (t, J = 6.6 Hz, 4H), 5.73 (s, 2H), 5.90 (m, 4H), 6.13 (m, 4H), 6.65 (m, 4H), 6.74 (d, J = 8.4 Hz, 2H), 7.20 (d, J = 2.4 Hz, 2H), 7.29 (dd, J = 2.4, 8.4 Hz, 2H), 8.05 ppm (s, 4H); ^{13}C NMR (150 MHz, $CDCl_3$): δ = 25.87, 29.15, 29.31, 29.49, 29.53, 38.03, 68.82, 106.85, 108.39, 113.02, 113.90, 116.89, 130.77, 131.66, 132.07, 133.41, 155.36 ppm; HRMS: m/z : calcd for $C_{42}H_{48}Br_2N_4O_2K$: 839.1975 [$M+K$] $^+$; found: 839.1628.

Synthesis of Por(Br)₄: Compound **1** (0.82 g, 1.43 mmol) and **2** (1.15 g, 1.43 mmol) were dissolved in $CHCl_3$ (1500 mL) and ethanol (11 mL) and the solution was purged with argon for 2 h. Boron trifluoride diethyl etherate (0.25 mL, 2.03 mmol) was added to the solution under light shielding, the mixture was stirred for 3 h at room temperature, and chloranil (1.2 g, 4.88 mmol) was added. The solution was further stirred at room temperature for 2 h. The obtained black solution was passed through silica gel and the filtrate was evaporated. The solid material was further purified by column chromatography (silica gel, hexane/chloroform = 2:1–1:1) to yield **Por(Br)₄** as a purple powder (0.46 g, 25%). M.p. 176–178 °C; 1H NMR (600 MHz, $CDCl_3$, TMS): δ = –2.86 (s, 2H), –0.13 (m, 8H), 0.09 (m, 16H), 0.15 (m, 8H), 0.89 (m, 8H), 3.90 (t, J = 5.1 Hz, 8H), 7.15 (d, J = 9.0 Hz, 4H), 7.84 (dd, J = 2.4, 9.0 Hz, 4H), 8.19 (d, J = 2.4, 4H), 8.77 ppm (s, 8H); ^{13}C NMR (150 MHz, $CDCl_3$): δ = 26.31, 27.19, 27.58, 28.68, 29.03, 69.04, 111.41, 112.95, 114.41, 132.40, 133.20, 137.62, 140.82, 158.52 ppm; MALDI-TOF-MS: m/z : calcd for $C_{68}H_{70}Br_4N_4O_4$: 1326.21; found: 1326.60.

Synthesis of Por(BT)₄: A mixture of **Por(Br)₄** (0.3 g, 0.23 mmol), 2,2'-bi-thiophene-5-boronic acid pinacol ester (0.39 g, 1.34 mmol), and sodium carbonate (0.51 g) in toluene (30 mL), ethanol (7.5 mL), and water (7.5 mL) was bubbled with argon for 1 h. Tetrakis(triphenylphosphine)-palladium(0) (10 mol %/**Por(Br)₄**) was added to the solution and the mixture was refluxed for 5 h. After cooling, the reaction mixture was washed with water and the organic layer was dried over sodium sulfate. The solvent was evaporated and the obtained solid was purified by column chromatography (silica gel, hexane/chloroform = 1:1–0:1) to give **Por(BT)₄** as a purple powder (0.17 g, 46%). M.p. 220–221 °C; 1H NMR (600 MHz, $CDCl_3$, TMS): δ = –2.59 (s, 2H), –0.20 (m, 8H), –0.13 (m, 8H), 0.13 (m, 16H), 0.95 (m, 8H), 3.95 (t, J = 5.1 Hz, 8H), 6.98 (dd, J = 3.6, 4.8 Hz, 4H), 7.14 (dd, J = 1.2, 3.6 Hz, 4H), 7.14 (d, J = 4.2 Hz, 4H), 7.17 (dd, J =

1.2, 4.8 Hz, 4H), 7.24 (d, J = 4.2, 4H), 7.29 (d, J = 9.0, 4H), 7.97 (dd, J = 2.4, 9.0 Hz, 4H), 8.38 (d, J = 2.4, 4H), 8.84 ppm (s, 8H); ^{13}C NMR (150 MHz, $CDCl_3$): δ = 25.78, 27.16, 27.35, 28.42, 28.89, 68.91, 111.87, 115.10, 122.93, 123.28, 124.05, 124.62, 125.26, 127.79, 132.04, 132.59, 135.78, 137.66, 143.29, 159.18 ppm; UV/Vis (dichloromethane): λ_{max} (ϵ) = 423 (5.1×10^5), 515 (3.2×10^4), 548 (1.2×10^4), 590 (1.2×10^4), 645 nm (6.0×10^3 mol $^{-1}$ dm 3 cm $^{-1}$); fluorescence (dichloromethane): λ_{em} (Φ_F) = 650 nm (0.023); MALDI-TOF-MS: m/z : calcd for $C_{87}H_{84}N_4O_5S_4$: 1392.53; found: 1393.72; MALDI-TOF-MS: m/z : calcd for $C_{100}H_{90}N_4O_4S_8$: 1667.48; found: 1668.51.

Synthesis of PorZn(BT)₄: Zinc acetate dihydrate (264 mg, 1.2×10^{-4} mol, 20 equiv/**Por(Br)₄**) in methanol (7.6 mL) was added to a solution of **Por(BT)₄** (100 mg, 6.0×10^{-5} mol) in $CHCl_3$ (38 mL; $CHCl_3$ /methanol = 5:1) and the solution was heated to reflux at 70 °C for 4 days. The reaction mixture was diluted with $CHCl_3$, washed with water, and dried over sodium sulfate. The solvent was evaporated and the obtained solid was purified by column chromatography (silica gel, hexane/chloroform = 1:1–0:1) to give **PorZn(BT)₄** as a pink powder (102 mg, quant.). M.p. 217–219 °C; 1H NMR (600 MHz, $CDCl_3$, TMS): δ = –0.33 (m, 16H), 0.05–0.88 (m, 16H), 0.95 (m, 8H), 3.96 (t, J = 5.4 Hz, 8H), 6.97 (dd, J = 3.6, 5.4 Hz, 4H), 7.13 (dd, J = 1.2, 3.6 Hz, 4H), 7.14 (d, J = 3.6 Hz, 4H), 7.17 (dd, J = 1.2, 4.2 Hz, 4H), 7.25 (d, J = 4.2 Hz, 4H), 7.29 (d, J = 8.4 Hz, 4H), 7.97 (dd, J = 2.4, 8.4 Hz, 4H), 8.38 (d, J = 2.4, 4H), 8.93 ppm (s, 8H); ^{13}C NMR (150 MHz, $CDCl_3$): δ = 25.55, 27.07, 27.28, 28.20, 28.77, 68.94, 111.96, 116.08, 122.88, 123.24, 124.03, 124.62, 125.19, 126.67, 127.78, 131.58, 132.44, 132.73, 135.71, 137.68, 143.40, 150.37, 159.20 ppm; UV/Vis (dichloromethane): λ_{max} (ϵ) = 425 (4.8×10^5), 549 (2.4×10^4), 585 nm (2.0×10^3 mol $^{-1}$ dm 3 cm $^{-1}$); fluorescence (dichloromethane): λ_{em} (Φ_F) = 653 nm (0.023); MALDI-TOF-MS: m/z : calcd for $C_{100}H_{90}N_4O_4S_8Zn$: 1729.38; found: 1730.82.

Zinc insertion for Por(Br)₄ and Por(OMe)₄: Because of the simplicity of the 1H NMR spectrum in the aromatic region, **Por(Br)₄** was used instead of **Por(BT)₄** to evaluate a zinc insertion reaction of a doubly strapped porphyrin. Zinc acetate dihydrate (83 mg, 3.8×10^{-4} mol, 10 equiv/**Por(Br)₄**) in methanol (7.6 mL) was added to a solution of **Por(Br)₄** (50 mg, 3.8×10^{-5} mol) in $CHCl_3$ (38 mL; $CHCl_3$ /methanol = 5:1), and the solution was heated to reflux at 70 °C. After a period of time (see Figure 2), a small amount of the reaction mixture was sampled and the solvent was evaporated. The solid materials were subjected to 1H NMR and absorption spectroscopic analysis without purification. In the case of **Por(OMe)₄**, the zinc insertion reaction was complete within 30 min at room temperature, as confirmed by absorption spectral change.

Film preparation and solid-state absorption and fluorescence spectral measurements: Solutions of the compounds in dichloromethane (2 mm) were spin-coated onto glass plates (1000 rpm for 20 s). Ten films were prepared for each compound and the absorption spectra were measured. The obtained FWHMs and peak shifts of the absorption spectra are given as average values and were reproducible within ± 1 nm. The fluorescence spectra of the spin-coated films were measured with the solid-sample holder for the Hitachi F7000 spectrophotometer and all the fluorescence intensities (see Figures S3 and S8 in the Supporting Information and Figure 4) were normalized by the optical densities of each film at the excitation wavelengths.

Acknowledgements

This work was partially supported by KAKENHI (No. 20750097) for K.S. and the “Nanotechnology Network Project” of the Ministry of Education, Culture, Sports, Science, and Technology Japan (MEXT). The authors thank Dr. K. Iozaki (NIMS) and R. Shomura (NIMS) for the mass spectral measurements. The authors are grateful to Prof. T. Konishi (Shibaura Institute of Technology), Dr. T. Nakanishi (MPI-NIMS International Joint Laboratory), and Dr. T. Ikeda (Kyushu University) for valuable comments.

- [1] *Handbook of Conducting Polymers*, (Eds.: T. A. Skotheim, J. R. Reynolds), Taylor & Francis, Milton Park, **2006**.
- [2] J. H. Burroughes, C. A. Jones, R. H. Friend, *Nature* **1988**, 335, 137.
- [3] J. H. Burroughes, D. D. C. Bradley, A. R. Brown, R. N. Marks, K. Mackay, R. H. Friend, P. L. Burns, A. B. Holmes, *Nature* **1990**, 347, 539.
- [4] N. C. Greenham, S. C. Moratti, D. D. C. Bradley, R. H. Friend, A. B. Holmes, *Nature* **1993**, 365, 628.
- [5] N. S. Sariciftci, L. Smilowitz, A. J. Heeger, F. Wudl, *Science* **1992**, 258, 1474.
- [6] G. Yu, J. Gao, J. C. Hemmelen, F. Wudl, A. J. Heeger, *Science* **1995**, 270, 1789.
- [7] S. Günes, H. Neugebauer, N. S. Sariciftci, *Chem. Rev.* **2007**, 107, 1324.
- [8] X. Yang, J. Loos, *Macromolecules* **2007**, 40, 1353.
- [9] A. P. Kulkarni, C. J. Tonzola, A. Babel, S. A. Jenekhe, *Chem. Mater.* **2004**, 16, 4556.
- [10] F. Hide, A. M. Díaz-García, B. J. Schwartz, A. J. Heeger, *Acc. Chem. Res.* **1997**, 30, 430.
- [11] J. Roncali, *Chem. Rev.* **1997**, 97, 173.
- [12] M. Kertesz, C. H. Choi, S. Yang, *Chem. Rev.* **2005**, 105, 3448.
- [13] Only the functionalized conducting polymer systems based on electrochemical polymerization are cited in ref. [14–36].
- [14] F. Bedioui, J. Devynck, C. Bied-Charreton, *Acc. Chem. Res.* **1995**, 28, 30.
- [15] T. Shimidzu, *Synth. Met.* **1996**, 81, 235.
- [16] B. Ballarin, S. Masiero, R. Seeber, D. Tonelli, *J. Electroanal. Chem.* **1998**, 449, 173.
- [17] M. Takeuchi, T. Shioya, T. M. Swager, *Angew. Chem.* **2001**, 113, 3476; *Angew. Chem. Int. Ed.* **2001**, 40, 3372.
- [18] M. Schäferling, P. Bäuerle, *J. Mater. Chem.* **2004**, 14, 1132.
- [19] K. Yamashita, M. Ikeda, M. Takeuchi, S. Shinkai, *Chem. Lett.* **2003**, 32, 264.
- [20] R. P. Kingsborough, T. M. Swager, *Angew. Chem.* **2000**, 112, 3019; *Angew. Chem. Int. Ed.* **2000**, 39, 2897.
- [21] T. Muto, T. Temma, M. Kimura, K. Hanabusa, H. Shirai, *Chem. Commun.* **2000**, 1649.
- [22] C.-C. You, P. Espindola, C. Hippus, J. Heinze, F. Würthner, *Adv. Func. Mater.* **2007**, 17, 3764.
- [23] C.-C. You, C. R. Saha-Möller, F. Würthner, *Chem. Commun.* **2004**, 2030.
- [24] J. L. Segura, R. Gomez, E. Reinold, P. Bäuerle, *Org. Lett.* **2005**, 7, 2345.
- [25] S. Chen, Y. Liu, W. Qiu, X. Sun, Y. Ma, D. Zhu, *Chem. Mater.* **2005**, 17, 2208.
- [26] T. Benincori, E. Brenna, F. Sannicoló, L. Trimarco, G. Zotti, P. Sozzani, *Angew. Chem.* **1996**, 108, 718; *Angew. Chem. Int. Ed. Engl.* **1996**, 35, 648.
- [27] B. Jusselme, P. Blanchard, E. Levillain, R. de Bettignies, J. Roncali, *Macromolecules* **2003**, 36, 3020.
- [28] G. Sonmez, C. K. F. Shen, Y. Rubin, F. Wudl, *Adv. Mater.* **2005**, 17, 897.
- [29] J. L. Reddinger, G. A. Sotzing, J. R. Reynolds, *Chem. Commun.* **1996**, 1777.
- [30] H. Brisset, A.-E. Navarro, C. Moustrou, I. F. Perepichka, J. Roncali, *Electrochem. Commun.* **2004**, 6, 249.
- [31] M. Catellani, S. Luzzati, N.-O. Lupsac, R. Mendichi, R. Consonni, A. Famulari, S. V. Meille, F. Giacalone, J. L. Segura, N. Martin, *J. Mater. Chem.* **2004**, 14, 67.
- [32] R. P. Kingsborough, T. M. Swager, *Adv. Mater.* **1998**, 10, 1100.
- [33] S. S. Zhu, R. P. Kingsborough, T. M. Swager, *J. Mater. Chem.* **1999**, 9, 2123.
- [34] L. Huchet, S. Akoudad, J. Roncali, *Adv. Mater.* **1998**, 10, 541.
- [35] H. C. Ko, S. Kim, H. Lee, B. Moon, *Adv. Func. Mater.* **2005**, 15, 905.
- [36] P.-L. Vidal, B. Divisia-Blohorn, G. Bidan, J. L. Hazemann, J.-M. Kern, J.-P. Sauvage, *Chem. Eur. J.* **2000**, 6, 1663.
- [37] K. Sugiyasu, T. M. Swager, *Bull. Chem. Soc. Jpn.* **2007**, 80, 2074.
- [38] T. M. Swager, *Acc. Chem. Res.* **1998**, 31, 201.
- [39] R. Jakubiak, C. J. Collison, W. C. Wan, L. J. Rothberg, *J. Phys. Chem. A* **1999**, 103, 2394.
- [40] M. Fujitsuka, A. Masuhara, H. Kasai, H. Oikawa, H. Nakanishi, O. Ito, T. Yamashiro, Y. Aso, T. Otsubo, *J. Phys. Chem. B* **2001**, 105, 9930.
- [41] L. M. Herz, C. Silva, R. H. Friend, R. T. Phillips, S. Setayesh, S. Becker, D. Marsitsky, K. Müllen, *Phys. Rev. B* **2001**, 64, 195203.
- [42] H.-H. Sung, H.-C. Lin, *Macromolecules* **2004**, 37, 7945.
- [43] A. P. Kulkarni, S. A. Jenekhe, *Macromolecules* **2003**, 36, 5285.
- [44] T. Konishi, A. Ikeda, M. Asai, T. Hatano, S. Shinkai, M. Fujitsuka, O. Ito, Y. Tsuchiya, J.-i. Kikuchi, *J. Phys. Chem. B* **2003**, 107, 11261.
- [45] F. Montilla, R. Esquembre, R. Gómez, R. Blanco, J. L. Segura, *J. Phys. Chem. C* **2008**, 112, 16668.
- [46] H. Imahori, *J. Mater. Chem.* **2007**, 17, 31.
- [47] H. Imahori, Y. Sakata, *Adv. Mater.* **1997**, 9, 537.
- [48] T. Konishi, M. Horie, T. Wada, S. Ogasawara, J.-i. Kikuchi, A. Ikeda, *J. Porphyrins Phthalocyanines* **2007**, 11, 342.
- [49] J. A. A. Elemans, N. R. van Hameren, R. J. M. Nolte, A. E. Rowan, *Adv. Mater.* **2006**, 18, 1251.
- [50] F. Wuerthner, M. S. Vollmer, F. Effenberger, P. Emele, D. U. Meyer, H. Port, H. C. Wolf, *J. Am. Chem. Soc.* **1995**, 117, 8090.
- [51] M. S. Vollmer, F. Würthner, F. Effenberger, P. Emele, D. U. Meyer, T. Stümpfig, H. Port, H. C. Wolf, *Chem. Eur. J.* **1998**, 4, 260.
- [52] T. Otsubo, Y. Aso, K. Takimiya, *J. Mater. Chem.* **2002**, 12, 2565.
- [53] J. W. Dirks, G. Underwood, J. C. Matheson, D. Gust, *J. Org. Chem.* **1979**, 44, 2551.
- [54] J. S. Lindsey, R. W. Wanger, *J. Org. Chem.* **1989**, 54, 828.
- [55] B. J. Littler, Y. Ciringh, J. S. Lindsey, *J. Org. Chem.* **1999**, 64, 2864.
- [56] B. Stäubli, H. Fretz, U. Piantini, W.-D. Woggon, *Helv. Chim. Acta* **1987**, 70, 1173.
- [57] S. Shanmugathan, C. Edwards, R. W. Boyle, *Tetrahedron* **2000**, 56, 1025.
- [58] M. Momenteau, C. A. Reed, *Chem. Rev.* **1994**, 94, 659.
- [59] C. Song, T. M. Swager, *Macromolecules* **2005**, 38, 4569.
- [60] A. Osuka, F. Kobayashi, K. Maruyama, *Bull. Chem. Soc. Jpn.* **1991**, 64, 1213.
- [61] F. Cacialli, J. S. Wilson, J. J. Michels, C. Daniel, C. Silva, R. H. Friend, N. Severin, P. Samorí, J. P. Rabe, M. J. O'Connell, P. N. Taylor, H. L. Anderson, *Nat. Mater.* **2002**, 1, 160.
- [62] R. S. Becker, J. S. de Melo, A. L. Macanita, F. Elisei, *J. Phys. Chem.* **1996**, 100, 18683.
- [63] M. J. Frampton, H. L. Anderson, *Angew. Chem.* **2007**, 119, 1046; *Angew. Chem. Int. Ed.* **2007**, 46, 1028.
- [64] D. J. Cardin, *Adv. Mater.* **2002**, 14, 553.
- [65] D. Lee, T. M. Swager, *Synlett* **2004**, 149.
- [66] Q. Zhou, T. M. Swager, *J. Am. Chem. Soc.* **1995**, 117, 7017.
- [67] Q. Zhou, T. M. Swager, *J. Am. Chem. Soc.* **1995**, 117, 12593.
- [68] J.-H. Wan, J.-C. Feng, G.-A. Wen, W. Wei, Q.-L. Fan, C.-M. Wang, H.-Y. Wang, R. Zhu, X.-D. Yuan, C.-H. Huang, W. Huang, *J. Org. Chem.* **2006**, 71, 2565.
- [69] C.-Q. Ma, E. Mena-Osteritz, T. Debaerdemaeker, M. M. Wienk, R. A. Janssen, P. Bäuerle, *Angew. Chem.* **2007**, 119, 1709; *Angew. Chem. Int. Ed.* **2007**, 46, 1679.

Received: March 3, 2009

Revised: March 13, 2009